Characterizing photonic crystal waveguides with an expanded *k*-space evanescent coupling technique

Michael W. Lee[1*], Christian Grillet[1], Christopher G. Poulton[2], Christelle Monat[1], Cameron L. C. Smith[1], Eric Mägi[1], Darren Freeman[3], Steve Madden[3], Barry Luther-Davies[3], and Benjamin J. Eggleton[1]

[1]*Centre for Ultrahigh-bandwidth Devices for Optical Systems (CUDOS), School of Physics, University of Sydney, Sydney, NSW 2006, Australia*
[2]*Centre for Ultrahigh-bandwidth Devices for Optical Systems (CUDOS), and Department of Mathematical Sciences, University of Technology, Sydney, P.O. Box 123, Broadway NSW 2007, Australia*
[3]*Centre for Ultrahigh-bandwidth Devices for Optical Systems (CUDOS), Laser Physics Centre, Australian National University, Canberra, ACT 0200, Australia*
[*]*Corresponding author: mlee@physics.usyd.edu.au*

Abstract: We demonstrate a direct, single measurement technique for characterizing the dispersion of a photonic crystal waveguide (PCWG) using a tapered fiber evanescent coupling method. A highly curved fiber taper is used to probe the Fabry-Pérot spectrum of a closed PCWG over a broad *k*-space range, and from this measurement the dispersive properties of the waveguide can be found. Waveguide propagation losses can also be estimated from measurements of closed waveguides with different lengths. The validity of this method is demonstrated by comparing the results obtained on a 'W1' PCWG in chalcogenide glass with numerical simulation.

OCIS codes: (130.5296) Photonic crystal waveguides; (130.2790) Guided waves; (060.2300) Fiber measurements

References and links

1. J.-M. Lourtioz, H. Benisty, V. Berger, J.-M. Gerard, D. Maystre, and A. Tchelnokov, *Photonic Crystals: Towards Nanoscale Photonic Devices* (Springer, 2005).
2. S. McNab, N. Moll, and Y. Vlasov, "Ultra-low loss photonic integrated circuit with membrane-type photonic crystal waveguides," Opt. Express **11**, 2927-2939 (2003).
3. T. F. Krauss, "Planar photonic crystal waveguide devices for integrated optics," Phys. Status Solidi (a) **197**, 688-702, (2003).
4. T. J. Karle, Y. J. Chai, C. N. Morgan, I. H. White, and T. F. Krauss, "Observation of pulse compression in photonic crystal coupled cavity waveguides," J. Lightwave Technol. **22,** 514-519 (2004).
5. A. Martinez, F. Cuesta, and J. Martí, "Ultrashort 2-D photonic crystal directional couplers," IEEE Photon. Technol. Lett. **15**, 694-696 (2003).
6. M. Soljačić, S. G. Johnson, S. Fan, M. Ibanescu, E. Ippen, and J. D. Joannopoulos, "Photonic-crystal slow-light enhancement of nonlinear phase sensitivity," J. Opt. Soc. Am. B **19**, 2052-2059 (2002).
7. M. Notomi, K. Yamada, A. Shinya, J. Takahashi, C. Takahashi, and I. Yokohama, "Extremely large group velocity dispersion of line-defect waveguides in photonic crystal slabs," Phys. Rev. Lett. **87**, 253902 (2001).
8. A. Gomez-Iglesias, D. O'Brien, L. O'Faolain, A. Miller, and T. F. Krauss, "Direct measurement of the group index of photonic crystal waveguides via Fourier transform spectral interferometry," Appl. Phys. Lett. **90**, 261107 (2007).
9. R. J. P. Engelen, T. Karle, H. Gersen, J. Korterik, T. Krauss, L. Kuipers, and N. van Hulst, "Local probing of Bloch mode dispersion in a photonic crystal waveguide," Opt. Express **13**, 4457-4464 (2005).
10. N. Le Thomas, R. Houdré, M. V. Kotlyar, D. O'Brien, and T. F. Krauss, "Exploring light propagating in photonic crystals with Fourier optics," J. Opt. Soc. Am. B **24**, 2964-2971 (2007).
11. M. Notomi, A. Shinya, K. Yamada, J. Takahashi, C. Takahashi, and I. Yokohama, "Structural tuning of guiding modes of line-defect waveguides of SOI photonic crystal slabs," IEEE J. Quantum Electron. **38**, 736-742 (2002).

#99146 - $15.00 USD Received 21 Jul 2008; revised 19 Aug 2008; accepted 19 Aug 2008; published 21 Aug 2008

12. X. Letartre, C. Seassal, C. Grillet, P. Rojo-Romeo, P. Viktorovitch, M. Le Vassor d'Yerville, D. Cassagne, and C. Jouanin, "Group velocity and propagation losses measurement in a single-line photonic-crystal waveguide on InP membranes," Appl. Phys. Lett. **79**, 2312 (2001).
13. J. C. Knight, G. Cheung, F. Jacques, and T. A. Birks, "Phase-matched excitation of whispering-gallery-mode resonances by a fiber taper," Opt. Lett. **22**, 1129-1131 (1997).
14. P. E. Barclay, K. Srinivasan, M. Borselli, and O. Painter, "Efficient input and output fiber coupling to a photonic crystal waveguide," Opt. Lett. **29**, 697-699 (2004).
15. P.E. Barclay, K. Srinivasan, M. Borselli, and O. Painter, "Probing the dispersive and spatial properties of photonic crystal waveguides via highly efficient coupling from fiber tapers," Appl. Phys. Lett. **85**, 4-6 (2004).
16. K. Srinivasan, P. E. Barclay, M. Borselli, and O. Painter, "Optical-fiber based measurement of an ultra-small volume high-Q photonic crystal microcavity," Phys. Rev. B **70**, 081306(R) (2004).
17. M. Fujii, C. Koos, C. Poulton, I. Sakagami, J. Leuthold and W. Freude, "A simple and rigorous verification technique for nonlinear FDTD algorithms by optical parametric four-wave mixing," Microwave Opt. Technol. Lett. **48**, 88-91 (2005).
18. C. Koos, M. Fujii, C. G. Poulton, R. Steingrueber, J. Leuthold, and W. Freude, "FDTD modelling of dispersive nonlinear ring resonators: accuracy studies and experiments," IEEE J. Quantum Electron. **42**, 1215-1223 (2006).
19. G. J. Pearce, T. D. Hedley, and D. M. Bird, "Adaptive curvilinear coordinates in a plane-wave solution of Maxwell's equations in photonic crystals," Phys. Rev. B, **71**, 195108 (2005).
20. C. Grillet, C. Monat, C. L. Smith, B. J. Eggleton, D. J. Moss, S. Frédérick, D. Dalacu, P. J. Poole, J. Lapointe, G. Aers, and R. L. Williams, "Nanowire coupling to photonic crystal nanocavities for single photon sources," Opt. Express **15**, 1267-1276 (2007).
21. D. Freeman, C. Grillet, M. W. Lee, C. L. C. Smith, Y. Ruan, A. Rode, M. Krolikowska, S. Tomljenovic-Hanic, C. M. De Sterke, M. J. Steel, B. Luther-Davies, S. Madden, D. J. Moss, Y. H. Lee, and B. J. Eggleton, "Chalcogenide glass photonic crystals," Photonics Nanostruct. Fundam. Appl. **6**, 3-11 (2008).
22. M. W. Lee, C. Grillet, C. L. C. Smith, D. J. Moss, B. J. Eggleton, D. Freeman, B. Luther-Davies, S. Madden, A. Rode, Y. Ruan, and Y. Lee, "Photosensitive post tuning of chalcogenide photonic crystal waveguides," Opt. Express **15**, 1277-1285 (2007).
23. E. Kuramochi, M. Notomi, S. Hughes, A. Shinya, T. Watanabe and L. Ramunno, "Disorder-induced scattering loss of line-defect waveguides in photonic crystal slabs," Phys Rev B. **72**, 161318 (2005).
24. S. Combrié, E. Weidner, A. DeRossi, S. Bansropun, S. Cassette, A. Talneau, and H. Benisty, "Detailed analysis by Fabry-Pérot method of slab photonic crystal line-defect waveguides and cavities in aluminium-free material system," Opt. Express **14**, 7353-7361 (2006).
25. D. Y. Choi, S. Madden, A. Rode, R. Wang, and B. Luther-Davies, "Fabrication of low loss $Ge_{33}As_{12}Se_{55}$ (AMTIR-1) planar waveguides," Appl. Phys. Lett. **91,** 011115 (2007).
26. J. Schrauwen, D. Van Thourhout, and R. Baets, "Focused-ion-beam fabricated vertical fiber couplers on silicon-on-insulator waveguides," Appl. Phys. Lett. **89**, 141102 (2006).
27. L. O'Faolain, T. P. White, D. O'Brien, X. Yuan, M. D. Settle, and T. F. Krauss, "Dependence of extrinsic loss on group velocity in photonic crystal waveguides," Opt. Express **15**, 13129-13138 (2007).
28. J. Li, T. P. White, L. O'Faolain, A. Gomez-Iglesias, and T. F. Krauss, "Systematic design of flat band slow light in photonic crystal waveguides," Opt. Express **16**, 6227-6232 (2008).

1. Introduction

Planar photonic crystals, which are formed by creating a periodic array of air holes in a thin dielectric slab, present an attractive platform for the development of compact optical devices. This is due to the ability to control light on the wavelength scale within defects in the lattice [1]. Waveguide defects are of interest both as interconnects for optical integrated circuits [2] and also as functional devices in their own right [3]. The broad ability to engineer the dispersion of these waveguides, due to the many degrees of freedom in their design, has led to applications in pulse compression [4], compact couplers [5] and broadband slow light waveguides for optical buffers and enhanced light/matter interaction [6].

Experimentally characterizing the dispersive properties of novel waveguide designs is an important step in realizing some of the potential applications of photonic crystal waveguides. Previously, several techniques have been employed including observation of Fabry-Pérot (FP) resonances in the transmission spectrum from photonic crystal/ ridge waveguide interfaces [7], analysis of fringes from an external Mach-Zehnder interferometer [8], phase sensitive near field microscopy [9] and Fourier optics techniques [10]; although those techniques have proven their ability to retrieve the dispersion curve, they require the presence of conventional index guiding access waveguides that 1) can limit the insertion efficiency unless an elaborate and multistep manufacturing process (such as inverse tapers [3, 11]) is employed, 2) can hinder the measurements due to coupling issues in the slow light regime between the photonic

#99146 - $15.00 USD Received 21 Jul 2008; revised 19 Aug 2008; accepted 19 Aug 2008; published 21 Aug 2008

crystal waveguide (PCWG) and the ridge waveguide. Another technique, based on observing FP resonances in the photoluminescence spectra of closed PCWGs has also been demonstrated [12]. This technique does not require access waveguides but relies on the use of internal emitters such as quantum wells or quantum dots, making it incompatible with passive structures. Evanescent coupling using a tapered fiber, which has been used to efficiently probe a variety of microphotonic devices [13], including PCWGs [14], has also been used to extract the dispersion properties without the need of integrated access waveguides [15]. However, this technique requires multiple measurements, while probing the structure with a variable taper diameter.

In this work we demonstrate a simple technique for characterizing the dispersion and group velocity of a photonic crystal waveguide that is based on tapered fiber evanescent coupling and that requires only a single spectral measurement. We measure the FP spectrum of a closed PCWG using a tapered fiber and, noting that the resonances are approximately equally spaced in reciprocal-space (*k*-space), we retrieve the dispersion of the waveguide, whose shape is in good agreement with simulation. This method crucially employs a taper with a small radius of curvature which leads to an increased coupling range in *k*-space. We also show that our approach can be used to estimate the waveguide propagation losses. Because it provides a quick and simple characterization of the waveguide spectral properties, our technique can assist the development of novel waveguide designs for dispersion engineering in photonic crystals without the need of integrated access waveguides or internal light sources.

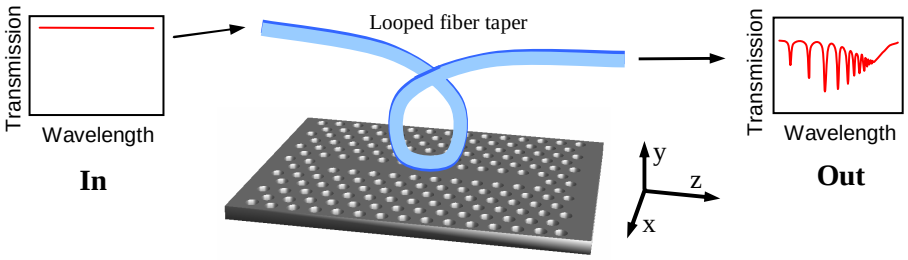

Fig. 1. A schematic of the setup used to characterize the photonic crystal waveguide. A highly curved taper is brought into close proximity with a closed photonic crystal waveguide and the transmission spectrum through the taper is monitored. Dips in the spectrum appear where light is coupled from the taper and into the waveguide.

2. Principle

Figure 1 summarizes the method that we propose for characterizing the dispersion and propagation loss of a PCWG. The figure depicts a highly curved fiber taper (~25μm radius of curvature) in close proximity to a closed PCWG. A closed waveguide, with photonic crystal mirrors at each end, forms a long linear cavity which supports Fabry-Pérot (FP) resonances based on the guided modes of the waveguide. Fiber tapers have been used to probe a range of microcavities including whispering gallery mode resonators [13] and photonic crystal resonators [16]. Here, the taper is used to excite the FP modes, which are observed as dips in the transmission spectrum of the taper since this is where optical power is coupled out of the taper and into the closed waveguide. The taper transmission spectrum allows us to measure the wavelengths and quality factors (*Q*) of the FP resonances.

2.1 Broadband evanescent coupling

Evanescent coupling between two modes can occur when they have the same frequency and are phase matched, i.e. when there is some overlap of their *k*-space distribution. This

#99146 - $15.00 USD Received 21 Jul 2008; revised 19 Aug 2008; accepted 19 Aug 2008; published 21 Aug 2008

translates into an overlap between the two modes on a band diagram. In the case of an infinitely long taper and waveguide there is only a single point of intersection between the two continuous dispersion curves. In contrast, using a highly curved taper results in an expanded *k*-space distribution of the taper mode at the plane of the sample, and a closed waveguide gives rise to a series of discrete FP resonances in place of the continuous waveguide dispersion curve. The bandwidth of coupling achieved depends on both the degree of *k*-space broadening of the taper mode and the average slope of the waveguide dispersion curve.

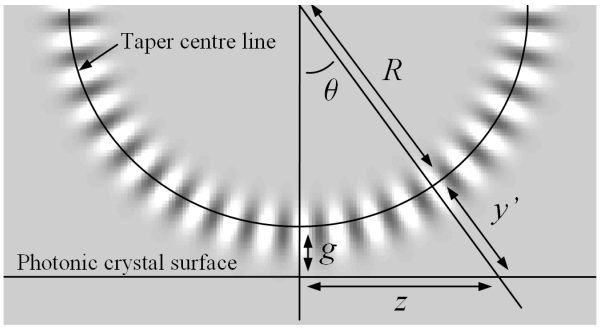

Fig. 2. The coordinate system used for mapping the fields of the curved taper onto the photonic crystal surface. The taper mode is shown for reference.

To illlustrate the underlying principle, we numerically examine the *k*-space extent of the curved taper mode and its overlap with the FP resonances of a closed W1 waveguide (a single row of holes removed in a triangular lattice). The extent of the curved-taper mode fields in the k_z direction can be calculated to a good approximation by directly mapping the fields from the coordinate system of the taper to that of a plane parallel to the photonic crystal. In doing so we assume that the curvature remains sufficiently small that the transverse mode profile is not significantly perturbed from that of a straight waveguide. If a field component of the uncurved taper mode is represented in local coordinates by *f(x',y')*, then the Fourier transform of the fields along the *z*-axis is given by:

$$\tilde{F}(k_z) = \int_{-\infty}^{\infty} f(0, \sqrt{z^2 + (R+g)^2} - R) \exp(i\beta R \arctan\frac{z}{R+g}) e^{-ik_z z} dz \qquad (1),$$

where β is the propagation constant of the taper at the waist, and the other variables are as shown in Fig. 2. This gives the *k*-space distribution of the curved taper mode in the *z*-direction at the photonic crystal surface. These calculations are summarized in Fig. 3(a), which plots the approximate size (to $1/e^2$) of the taper mode *k*-space distribution as a function of the radius of curvature. The taper waist was 0.8μm and the wavelength considered was 1550nm. The *k*-space extent, and hence the ability to characterize the PCWG, clearly increases as the curvature radius is reduced.

The resonances of the closed waveguide were computed using a finite-difference time domain (FDTD) algorithm [17], implemented on a large parallel cluster. The frequencies of the resonances for an 80 period W1 type closed waveguide were found by examining the spectral response of the structure to a broadband excitation. The mode fields were then computed at the resonant peaks and the spatial frequencies of the modes along the waveguide axis were evaluated numerically. The computational demands of simulating such a large structure meant that the modes in the slow group velocity band edge (beyond $k_z \sim 0.4$) could not be accurately calculated. Thus we used plane wave expansion calculations for comparison with our experimental results. The result of these calculations is summarized in Fig. 3(b), which shows the expanded *k*-space distribution of the curved taper mode and its overlap with the discrete FP resonances. On the same graph we show the dispersion curve of the fundamental waveguide mode, as calculated using the plane-wave method. The discrepancy

#99146 - $15.00 USD Received 21 Jul 2008; revised 19 Aug 2008; accepted 19 Aug 2008; published 21 Aug 2008

between the two curves is due to the limitations in discretization of the two methods [18, 19]; we can nevertheless see from this graph that the resonances of the complete structure lie to a good approximation on the dispersion curve of the infinite waveguide. We also observe that using a highly-curved taper allows a large portion of the PCWG dispersion curve to be probed in a single measurement (>50% of the *k*-space below the light line at telecommunications wavelengths).

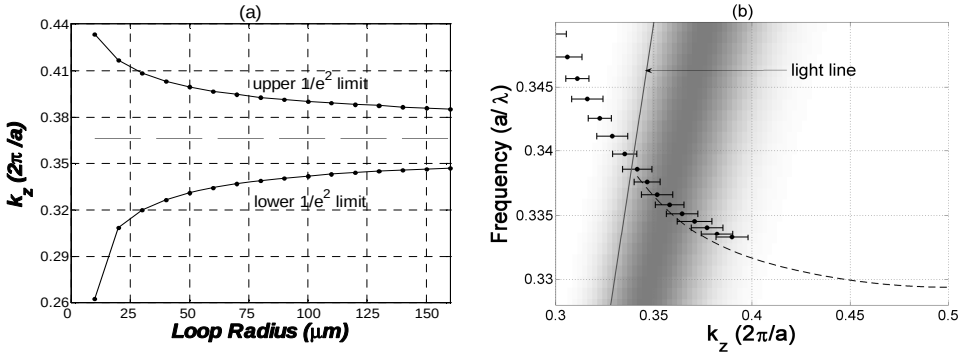

Fig. 3. (a). The *k*-space interval (to $1/e^2$ of the peak) covered by the curved taper mode as a function of the radius of curvature. Here, the taper waist diameter is 0.8μm and the wavelength is 1550nm. (b). The case of a tightly looped taper (47μm loop diameter) and closed waveguide. The k-space distribution of the taper mode is shown by the shaded region and the FP modes of the closed waveguide are represented by the points and horizontal bars, which show the approximate *k*-space extension of the modes. The dashed line is a plane wave calculation of the waveguide mode.

2.2 Characterizing the dispersive properties

The dispersive properties of the PCWG can be obtained by measuring the wavelengths of the FP resonances in the closed waveguide. If we assume that there is no phase change upon reflection from the cavity ends (effectively ignoring the penetration depth into the bulk photonic crystal region), then the *k*-space interval between each successive resonance is $\Delta k = 2\pi/2l$, where l is the length of the closed waveguide. The dispersion curve of the waveguide mode may be reconstructed with the following procedure: the wavelengths of the resonances are converted to reduced frequency, $f = a/\lambda$, where a is the lattice constant of the photonic crystal, then these frequencies are plotted in order with a spacing of Δk. This provides a reconstruction of the waveguide dispersion curve, however the absolute wavevector must be estimated by knowledge of the taper *k*-space distribution or by comparison with simulation.

The group velocity of the PCWG mode as a function of wavelength may be estimated by measuring the free spectral range (FSR) between the FP resonances and applying the formula;

$$\frac{v_g}{c} = \frac{2l\Delta\lambda_{FSR}}{\lambda_0^{\,2}} \qquad (2),$$

where $\Delta\lambda_{FSR}$ is the free spectral range between two adjacent resonances and λ_0 is the central wavelength between the resonances. This method is similar to those presented in Refs. [7, 12], however, in those works either an internal light source, or free space coupling is required to excite the FP modes.

2.3 Characterizing propagation loss

Examination of the *Q*-factors and coupling strengths of the FP resonances can give us a direct estimate of the photon lifetime in the closed waveguide and thus an estimate of the propagation losses. In our particular case, and for moderately slow group velocities, the derived intrinsic *Q* can be related to two sources of losses: the propagation losses (including

#99146 - $15.00 USD Received 21 Jul 2008; revised 19 Aug 2008; accepted 19 Aug 2008; published 21 Aug 2008

both absorption and scattering loss) and out of plane radiation losses incurred at the cavity terminations (R<1, where R is the intensity reflectivity). It follows [12]:

$$\frac{2\pi}{\lambda Q} = \frac{\alpha_{prop}}{n_g} + \frac{1-R}{n_g L} \tag{3}$$

By comparing the *Q* obtained from different cavity lengths, one can determine the reflection at the closed waveguide ends and therefore extract the propagation losses as a function of wavelength and group velocity.

3. Experimental setup

The experimental setup used in this work consisted of a nanopositioning stage, a looped fiber taper and a spectral measurement system, made up of a broadband light source (Erbium ASE) and an optical spectrum analyzer (Agilent 86140B set to 60pm resolution bandwidth). The nanopositioning stage could be used to control the position of the taper in increments of ~100nm and we were able to align the taper with the waveguide leaving a small air gap between them. Due to some mechanical flexibility in the taper and the presence of attractive forces between the taper and the sample, estimating the size of the gap was difficult. All measurements, unless otherwise noted, were made with the taper out of contact with the sample. A linear polarizer was set so that the light in the taper was TE polarized at the sample.

The tapers used in this work were created by flame brushing and elongating a standard single mode (at 1550nm) fiber using the technique described in [20]. The loop was formed by introducing some slack into the taper and applying a twist to form the loop. The loop was then tightened by removing most of the slack from the taper. The resultant tapers have waist diameters ~0.8μm with a typical loop radius of ~25μm.

The test photonic crystal sample was fabricated in AMTIR-1 ($Ge_{33}As_{12}Se_{55}$) glass by focused ion beam (FIB) milling using the method described in [21]. The target parameters for the lattice were a period of 520nm, a hole radius of 0.3 times the period and a slab thickness of 300nm. In addition to the AMTIR-1 membrane there was also a 30nm thick Si_3N_4 layer on the side of the membrane closest to the taper. The nominal refractive index for the thin film, ultrafast pulsed laser deposited, AMTIR-1 layer was 2.68. Waveguides were formed in the lattice by removing a single row of holes and closed waveguides were available with 80, 120 and 160 holes removed (cavity lengths of 41.6μm, 62.4μm and 83.2μm respectively). There were 21 rows of holes on each side of the waveguides and 20 at each of the ends.

#99146 - $15.00 USD Received 21 Jul 2008; revised 19 Aug 2008; accepted 19 Aug 2008; published 21 Aug 2008

4. Results and discussion

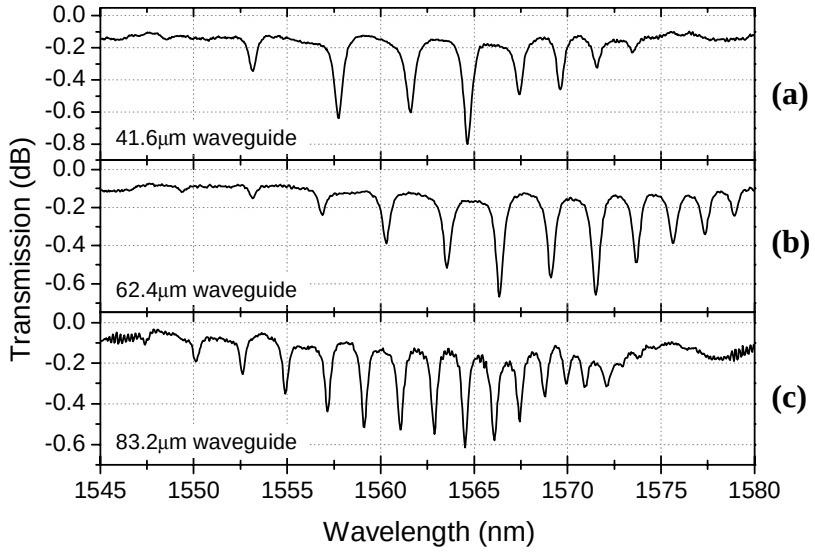

Fig. 4. The coupling spectra obtained for each of the three lengths of closed waveguide. Dips represent coupling to the FP modes of the closed waveguide.

The evanescent coupling spectrum for each of the three waveguide lengths is shown in Fig. 4. Each spectrum exhibits a series of dips which correspond to the FP resonances of the closed waveguides. The taper loop radius was ~40μm and the waist diameter was ~0.8μm for these measurements. As expected, the average FSR decreased for longer closed waveguides. To confirm that the resonances we observe are related to the closed waveguide, and not to the taper, we measured the coupling spectra of the 160 hole closed waveguide using two different looped tapers. Figure 5 shows the spectra obtained with the two tapers, taper 1 corresponds to the taper used above, while taper 2 had a loop radius of ~24μm and a waist diameter of ~0.8μm. In both traces the FP resonances occur at the same wavelengths, although the smaller loop diameter of taper 2 allowed it to couple over a larger wavelength range, as predicted in section 2.1. In this case the measurement with taper 2 was taken with the taper in contact with the sample, however, no difference in the coupling range was observed with the taper in or out of contact.

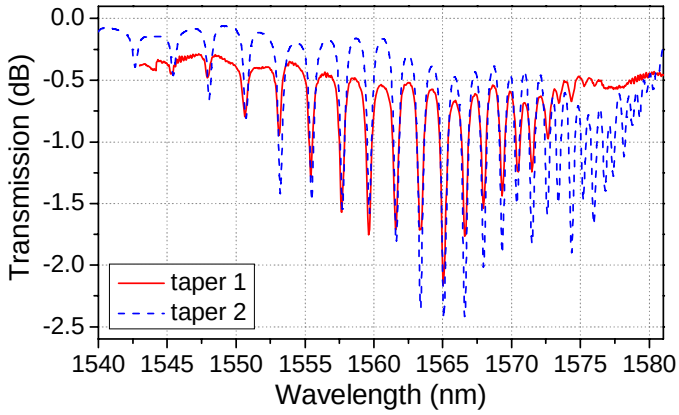

Fig. 5. The coupling spectra obtained for the 160 hole closed waveguide using two different looped tapers. The FP resonances appear at the same wavelengths in each case.

#99146 - $15.00 USD Received 21 Jul 2008; revised 19 Aug 2008; accepted 19 Aug 2008; published 21 Aug 2008

To demonstrate the reconstruction of the PCWG dispersion curve, we take the data from taper 2 in Fig. 5 and apply the method described in section 2.2. The resulting dispersion curve is shown in Fig. 6(a). The shape of the experimentally retrieved curve shows a good match with the simulated curve. The simulation parameters were the same as the sample target parameters, except the radius of the holes was reduced to 0.28a. We believe that this lies within the uncertainty for the real fabricated samples. The simulation was performed using the RSoft bandSOLVE program, which uses the plane wave expansion method.

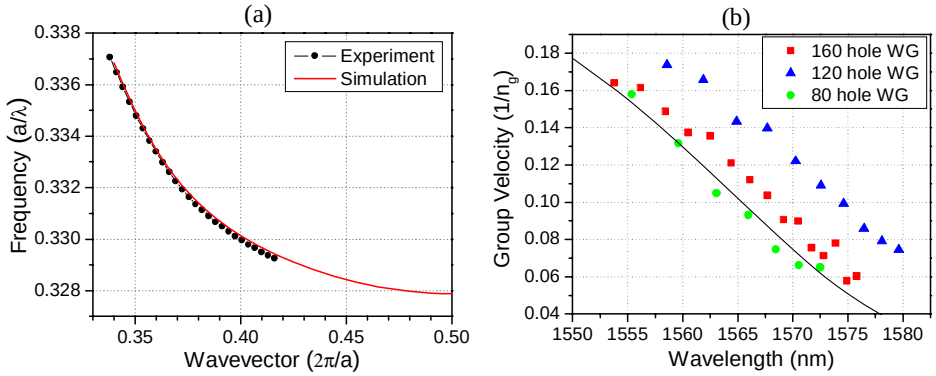

Fig. 6. (a). Comparison between the experimentally reconstructed dispersion curve of the W1 waveguide, and a plane wave simulation for that system. The absolute wavevectors for the experimental curve were determined by matching the small *k* values with simulation. (b) Comparison of the experimentally obtained group velocity for each of the three lengths of waveguide with a plane wave simulation (continuous line).

The group velocity of the waveguide mode as a function of wavelength was evaluated for each of the three waveguide lengths using Eq. (2). The wavelengths of the FP resonances were taken from Fig. 4 and the results for the group velocities are plotted in Fig. 6(b). The obtained group velocities show good agreement with the simulated curve, where the slope of each data set matches the simulation well. The measured group velocity varied in an approximately linear fashion with wavelength from approximately c/5 to c/20. The offset between the different waveguide lengths may be explained by small variations between the parameters of each sample, e.g. refractive index due to photosensitive processes [22]. The simulation data is the same as for the dispersion curve in Fig. 6(a).

Figure 7(a) shows the intrinsic *Q* [20] obtained for the closed waveguide samples with respectively 80 and 160 holes removed. By using Eq. (3) and comparing the two lengths of closed waveguide, the propagation loss was estimated as shown in Fig. 7(b). Propagation losses ranging from about 130dB/cm for a n_g of 8 till 370 dB/cm for a n_g of 20 can be estimated. Those values are far from state of the art values obtained in Si [23] or GaAs [24] PCWGs. The lower refractive index of the AMTIR-1 compared to Si or GaAs can not explain this discrepancy on its own. Measurements on bulk glasses indicate that the intrinsic loss of AMTIR-1 at 1550nm is around 0.1 dB/cm and low propagation losses down to 0.3 dB/cm were obtained in rib AMTIR-1 waveguides fabricated using a photolithography and plasma etching process [25] ruling out the AMTIR-1 as responsible for these large propagation losses. Extrinsic scattering losses (due to surface irregularities and non homogeneity) are believed to play a negligible role in those losses, especially considering the high degree of quality of these structures (smooth sidewalls, uniform lattice [21]). We are still investigating the cause of these enhanced losses but a possible explanation may be increased absorption resulting from incomplete removal of the carbon layer used to prevent charge build up during FIB milling, or alternatively undesired Ga implantation resulting from FIB milling [26]. Note that in Ref. [26], large optical losses on the order of 1dB/μm have been reported in 220 nm thick Si

#99146 - $15.00 USD Received 21 Jul 2008; revised 19 Aug 2008; accepted 19 Aug 2008; published 21 Aug 2008

waveguide gratings milled with a FIB (resulting in Ga ion implantation), about four orders of magnitude larger than that for non-implanted waveguides. The losses measured in our sample, however, should not be considered as an intrinsic limitation of PCWGs in chalcogenide glasses. Despite the high propagation losses, believed to be dominated by absorption, one can notice the expected increase of the propagation losses with n_g. Interestingly the loss trend seems to follow an $n_g^{\,b}$ dependence with $1<b<2$ in line with previous recent reports [27].

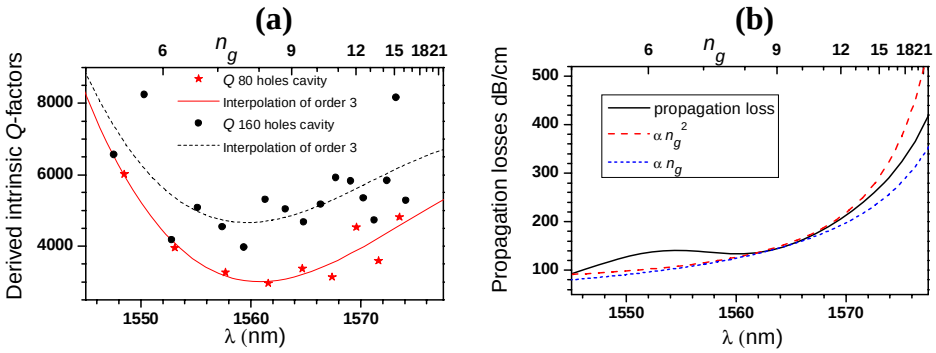

Fig. 7. (a). Comparison between the intrinsic Q-factor obtained with an 80 holes removed closed waveguide and a 160 holes removed closed waveguide as a function of wavelength and group index. (b). Propagation losses obtained using Eq. (3). The blue curves correspond to hypothetical losses that would respectively be characterized by a n_g and n_g^2 dependence.

For both the reconstruction of the dispersion curve and the determination of the group velocity we observed a good agreement between the experimental data and simulation; however we were not able to access the very low group velocity region of the dispersion curve near the mode cutoff. We do not believe this to be a fundamental limitation of the technique; rather it was a limitation for the particular tapers used in this experiment. A taper with a smaller bending radius and appropriate waist dimension should be able to probe further towards the cut-off. In addition, the sample we used had a large loss, which resulted in relatively wide resonances, so closely spaced peaks near the cut-off region were difficult to resolve.

5. Conclusion

In conclusion, we have demonstrated a fast, single measurement technique that allows for measuring the dispersion and group velocity of a photonic crystal waveguide. The method is based on evanescent coupling via a highly curved fiber taper which provides the basis for a broadband characterization of the waveguide. Both the dispersion and group velocity curves are in good agreement with numerical simulations. Although this technique requires dedicated test structures (closed waveguides), the requirement for only a single spectral measurement per waveguide makes it attractive for systematically and directly characterizing the full properties (dispersion and losses) of the PCWG without the use of integrated access waveguides or internal light sources which may affect the PCWG signature. This technique could be advantageous for rapidly probing novel waveguide designs that are developed, for instance, in the context of slow light dispersion engineering (such as in Ref. [28]) without the need for enhancing the coupling into the slow light regime.

Acknowledgments

This work was produced with the assistance of the Australian Research Council under the ARC Federation Fellowship and Centres of Excellence programs. CUDOS (the Centre for Ultrahigh-bandwidth Devices for Optical Systems) is an ARC Centre of Excellence.

#99146 - $15.00 USD Received 21 Jul 2008; revised 19 Aug 2008; accepted 19 Aug 2008; published 21 Aug 2008